Perspectives on instrumentation development for chemical species tomography in reactive-flow diagnosis

Perspectives on instrumentation development for chemical species tomography in reactive-flow diagnosis

Chang Liu[1], Hugh McCann[1], Lijun Xu[2]

1. School of Engineering, University of Edinburgh, Edinburgh EH9 3JL, U.K.
2. School of Instrumentation and Optoelectronic Engineering, Beihang University, Beijing 100191, China.

Abstract: Chemical species tomography (CST) has been deployed in a wide range of applications in the last two decades for multi-dimensional measurement of gaseous flow fields. CST offers unique capability for spatiotemporally resolved imaging of multiple thermochemical parameters. It is fundamentally robust, highly sensitive, and adaptable to industrial processes and large-scale combustion systems. The instrumentation methods used to implement CST measurements are critical in determining the physical and chemical variables that may be imaged by CST. In this perspective, we have three main objectives: a) discuss recent advances in CST instruments from the viewpoint of optics and electronics; b) highlight the on-going challenges for systems to address the ever-increasing requirements on temporal and spatial resolutions; and c) consider potential developments for next-generation CST instrumentation.

1 Introduction

Among the various laser-based sensing modalities, Chemical Species Tomography (CST), utilising chemical species-dependent photon absorption, offers unique capability for quantitative and spatiotemporally resolved imaging of thermochemical parameters in reactive flows, e.g., species concentration, temperature, pressure, velocity [1-3]. CST is implemented in a manner analogous to X-ray tomography with the difference that, wavelength-specified incident laser beams are used rather than X-rays to acquire the absorption measurements, i.e., projection data in tomography. In comparison with other popular two/three-dimensional imaging techniques for flow-field diagnosis, such as Planar/Volumetric Laser Induced Fluorescence (P/VLIF) [4, 5], emission imaging/tomography [6, 7] and Particle Image Velocimetry (PIV) [8], CST is the only technique that has gained widely environment-adaptive and industrial-oriented applications, ranging from lab-scale flame characterization to the very large-scale plume monitoring. It is important to note that some authors call CST by different names, such as laser absorption spectroscopy (LAS) tomography and tomographic absorption spectroscopy (TAS). We continue to use the name CST in order to emphasise that all the target variables are accessed by exploiting spectroscopic absorption by selected chemical species.

Since the first experimental demonstration of CST on gaseous hydrocarbon imaging [9], significant advances have been made from both the computational aspect, i.e., image reconstruction algorithms, and the instrumentational aspect, i.e. the design of measurement methods and data acquisition systems. Efforts expended on both of these aspects are aimed at characterising the target flows with better accuracy, speed and robustness. Computational efforts are nontrivial, involving the selective use of *a priori* information concerning the target flows (e.g. time-dependent flow evolution and grid-dependent flow smoothness). Various CST image reconstruction algorithms have been developed using algebraic techniques [10], regularisation [11], statistical inversion [12], optimisation [13], and most recently machine/deep-learning methods [14-16]. On the other hand, the instrumentational development of CST, such as novel opto-electronics design, plays a more essential and critical role by providing fundamentally new access to first-hand experimental data [1]. Depending on the nature of the target processes and the end users' requirements, CST instruments need to be customised to guarantee that the experimental data sampled for subsequent image reconstruction are physically meaningful and

reliable. Therefore, the first aim of this perspective is to chart the new advances and milestones in CST instrumentational development that cover real-world application of this technology.

For both lab-scale and industrial applications of CST, the specifications of spatial resolution and temporal resolution place ever more demanding requirements on the performance of CST instruments. To be concrete, the spatial resolution reflects how much detail of the target flow can be revealed by the tomographic images [17-19]. This factor is critically important for characterising flame structures and local hot spots that indicate combustion instabilities and thermodynamic behaviours of target flows. The temporal resolution indicates directly the extent to which variations of the target flow can be characterised. When monitoring turbulent flows, the temporal resolution needs to be set to a very high level, e.g., hundreds or thousands of frames per second (fps), depending on the turbulent frequency in question [20, 21]. However, improvement of the spatiotemporal resolution has been found to be very challenging for the deployment of CST in practical flows.

As CST is a hard-field tomography in nature [1], the fundamental prerequisite for better spatial resolution is to acquire more densely and evenly distributed spatial samples in the sensing region [22] (or the sinogram plot [23]). A straightforward attempt, similar to X-ray tomography, is to rotate the laser beams or the target objects for spatial sampling from more angular projections. This is suitable for monitoring static or quasi-static flames. However, the mechanical translation results in low-speed imaging, and therefore makes its implementation ineffective for characterising any dynamic features in turbulent flows; moreover, mechanical translation is incompatible with the environment within which many practical processes have to be operated. In contrast, fixed-beam CST sensors are preferred for high-speed monitoring where the absorbance from all the laser beams can be measured simultaneously, and gaining the necessary optical access to practical processes is then a fundamental step in system design for any given application. To maximise the temporal resolution of fixed-beam CST sensors, high-speed and multi-channel data acquisition and communication hardware electronics must work along with the optical sensor. However, the complexity and high cost in optics and electronics design, and the heavy data load for real-time multi-beam sensing, pose challenges that place CST instruments out of reach for many researchers in process engineering. In this perspective article, we will highlight these current challenges in order to identify recent progress, to propose potential solutions and project the CST instrumentational development challenge into the future.

The remainder of the article is organised as follows: Section 2 briefly reviews the latest development of CST optics, categorised by the above-mentioned scan-beam and fixed-beam sensors. Section 3 notes the most representative schemes of CST data acquisition, with their advantages and disadvantages. Section 4 will address the challenges inherent in the quest for better spatiotemporal resolution, and along the way, its impact on real-world CST applications. The overall perspective is summarised in Section 5 with an outlook on how CST instruments may be developed in the future.

2 Optics

Development of CST optical sensors, as a core part of CST instrumentation, has attracted many recent efforts to enhance penetrating spatiotemporal resolution. From the perspectives of opto-mechanics deployment, existing CST optical sensors can be categorised as scan-beam or fixed-beam sensors. In this section, we will address the most recent progress on the two categories by highlighting their suitability to various combustion scenarios and their limitations.

2.1 Scan-beam sensors

The objective of beam scanning in CST sensing is to increase the number of line-of-sight (LOS) LAS measurements, angularly and/or linearly, in the sensing region. The scan, mostly in a mechanical manner, is achieved by rotating/translating either the laser beams [24-26] or the subject [27-29]. From

the perspective of tomographic image reconstruction, the increased number of measurements can alleviate the rank deficiency of the CST inverse problem [1], thus improving the quality of the reconstruction with better accuracy and fewer artefacts. Fig. 1 shows state-of-the-art scan-beam CST sensors that have been demonstrated on imaging one-dimensional (1D) [27, 30, 31], two-dimensional (2D) [24, 25, 29, 32, 33] and three-dimensional (3D) laminar flames [26, 28]. For example, the 1D CST method shown in Fig. 1(a) is applied for recovering parameters from axisymmetric or rotationally symmetric flames using Abel inversion [27]. 2D CST can be either the extension of 1D CST in the vertical direction shown in Fig. 1(b) [29] or a cross-sectional reconstruction of a non-symmetric field, as shown in Fig. 1(c) [24]. 3D CST, as shown in Fig. 1(d) is referred to as a volumetric reconstruction of the target flow [28].

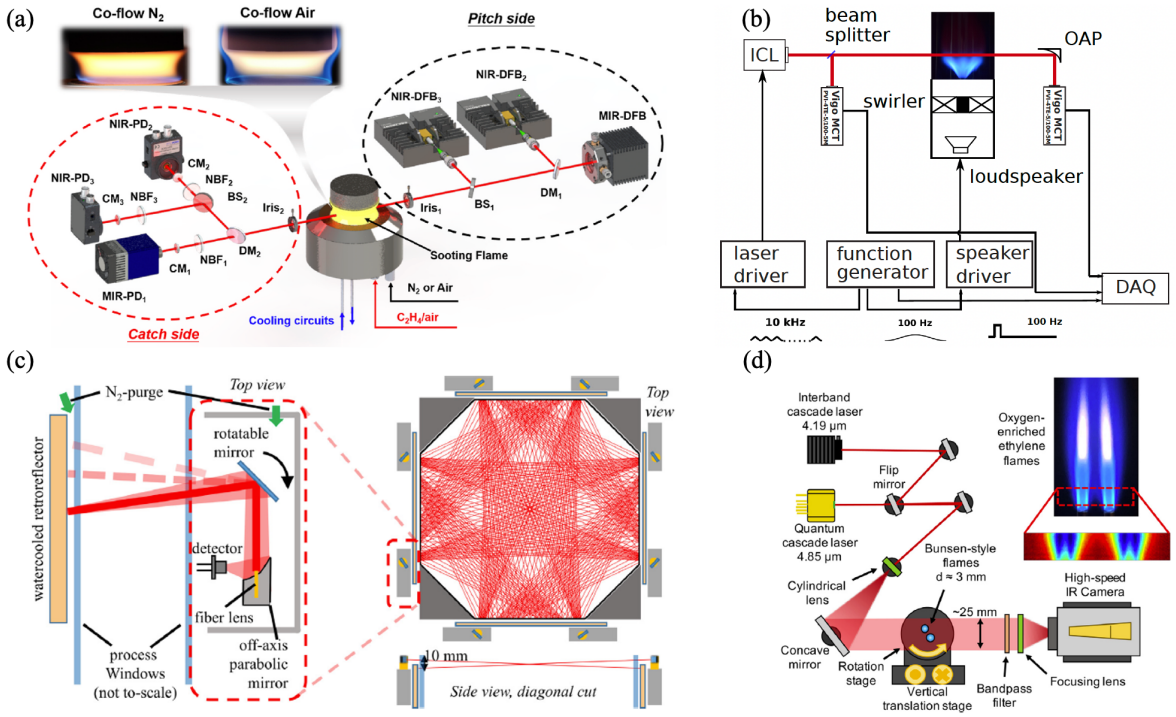

Fig. 1 State-of-the-art scan-beam CST sensors demonstrated for imaging of combustion processes: (a) 1D [27]; (b) vertical 2D [32]; (c) horizontal 2D [24]; and (d) 3D [28]. Reproduced from [24, 27, 28] with permission from Elsevier and Copyright Clearance Center. Reprinted with permission from [32] © The Optical Society.

Although more spatial samples can be obtained by the above sensors, the relatively low-speed mechanical scan of the laser beams can hardly reveal the dynamics of the target flow. Some attempts have been made by increasing the laser scanning speed, for example, introducing high-speed galvo mirrors and electro-optic beam deflectors [34]. However, the beam-scan strategy, limited by its nature of asynchronous sampling of the laser beams, is unable to capture the dynamic feature of the target flows. Therefore, scan-beam CST sensors are effective, in principle, only if the target flows to be reconstructed are static or quasi-static (i.e. statistically static). Furthermore, implementation of the beam scan requires full optical access of the target flows, and thus is impractical to be deployed on industrial combustors with very limited availability of optical windows.

Despite the above limitations, scan-beam CST sensors are effective in fundamental combustion research, for example, characterising axial and radial profiles [35], boundary effect [36], and non-uniformity [37] of the lab-scale flames. It is worth noting that single-beam LAS to measure multiple transitions or broadband spectra can also indicate the line-of-sight non-uniformity of gas parameters [38, 39]. However, it can hardly indicate axis-symmetrically resolution without *a priori* spatial information [40-43]. From the perspective of CST instrumentational development, scan-beam sensors can pave the way for designing fixed-beam sensors (see section 2.2). Concretely, beam scanning can provide proof-of-

concept validation of the CST capability in a low-cost and low-risk manner. This enables characterisation of multiple critical factors, such as detection limits of gas molecules on specific laser paths, optimised beam arrangements, signal-to-noise ratios of tomographic measurements and averaged spatial variation of the gas parameters, before fixed-beam sensors are designed. Considering the high cost and high complexity of fixed-beam CST sensors, the above approach could be a de-risking step to alleviate uncertainties of system design.

In addition, beam scanning may be the only option, to date, for CST at mid-infrared (MIR) wavelengths [25, 29, 44, 45]. Some chemical species, such as NOx, SOx, CO, are of particularly interest to the combustion community, but their absorption features at near-infrared (NIR) wavelengths are too weak to be measured with good signal-to-noise ratios (SNRs). Although the absorption of these pollutant species is much stronger at MIR wavelengths, transferring CST from NIR to MIR is extremely challenging due to the much-reduced availability of reliable fibre-coupled optical delivery. Assisted by high-speed motors, MIR cameras with micrometre-level or even smaller-size pixel arrays have been recently used to capture the two-dimensional laser light [45, 46]. As shown in Fig. 2, such tomographic systems are superior for achieving good spatial resolution, in streamwise dimension, to characterise the small-size structure and profile of some dynamic flames at MIR wavelengths. When applying them to an industrial environment, special care should be taken to avoid mechanical vibrations, which can misalign the optical setup and introduce oscillations in the light intensity imaged by a given pixel. Moreover, the dynamic response and linearity of sensing pixels should be carefully modelled as they can potentially cause saturation and distortion of the transmission signals and thus yield inaccurate measurements for CST.

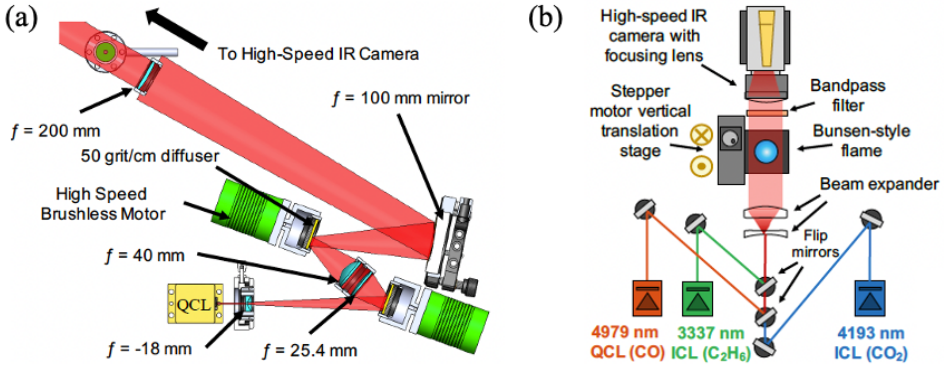

Fig. 2 State-of-the-art camera-assisted scan-beam sensors for MIR CST imaging in streamwise dimension, demonstrated for imaging of: (a) CO mole fraction at 4.8 μm using a Quantum Cascade Laser (QCL) and flame temperature with 0.1 s temporal resolution and 140 μm spatial resolution [46]; (b) CO at 4.97μm using a QCL, C_2H_6 at 3.34 μm and CO_2 at 4.19 μm using two Interband Cascade Lasers (ICLs) in an axisymmetric laminar flame with ~50 μm spatial resolution in the horizontal direction and ~125 μm in the vertical direction [45]. Reprinted with permission from [45, 46] © The Optical Society.

2.2 Fixed-beam sensors

The fixed/static-beam sensor approach, mostly implemented for 2D imaging, can maximise the temporal resolution of CST, as it enables parallelism from the perspective of optical sensing. Compared with scan-beam sensors that can only obtain spatially and temporally averaged reactive-flow characteristics, fixed-beam sensors are capable of imaging dynamic flows instantaneously at moderate/high frequencies, e.g., from hundreds of Hz to tens of kHz. As there are no moving parts in the fixed-beam sensor approach, it is a very robust method for monitoring combustion processes in harsh environments that are commonly coupled with acoustic noises and mechanical vibrations. To date, fixed-beam CST sensors have been pioneered in a range of industrial applications: on small-scale targets, e.g., IC engine combustion chambers [47-49] and heavy duty diesel engine [50]; mid/pilot-scale targets, e.g., wind tunnel/shock tube [51] and swirl combustors [52]; large-scale targets, e.g. power plant reactors [53, 54]; and most recently, super-large scale targets, e.g. civil aero engine exhaust [55].

A critical factor of fixed-beam CST sensor design is the layout of the laser beams, which determines physically the sensitivity of absorption measurement in the region of interest (ROI). In general, there are two manners of beam arrangements, a) regular with equi-angular projections and equi-spaced samples within each angular projection and b) irregular with optimised spatial samples in the ROI [23, 56]. It is worth noting that the regular beam arrangement contributes to uniformly distributing the sampling deficiency across the ROI. Therefore, given no/insufficient *a priori* information of the target, the regular beam arrangement is normally preferred over irregular ones for CST image reconstruction, unless that would lead to drastic under-sampling in the angular dimension [23]. Fig. 3 shows the state-of-the-art fixed-beam CST sensors that have been applied in the industry with (a, b) parallel-beam [15, 57], (c, d) fan-beam [51, 52, 58, 59, 60] and (e) irregular-beam arrangements [23, 47], respectively.

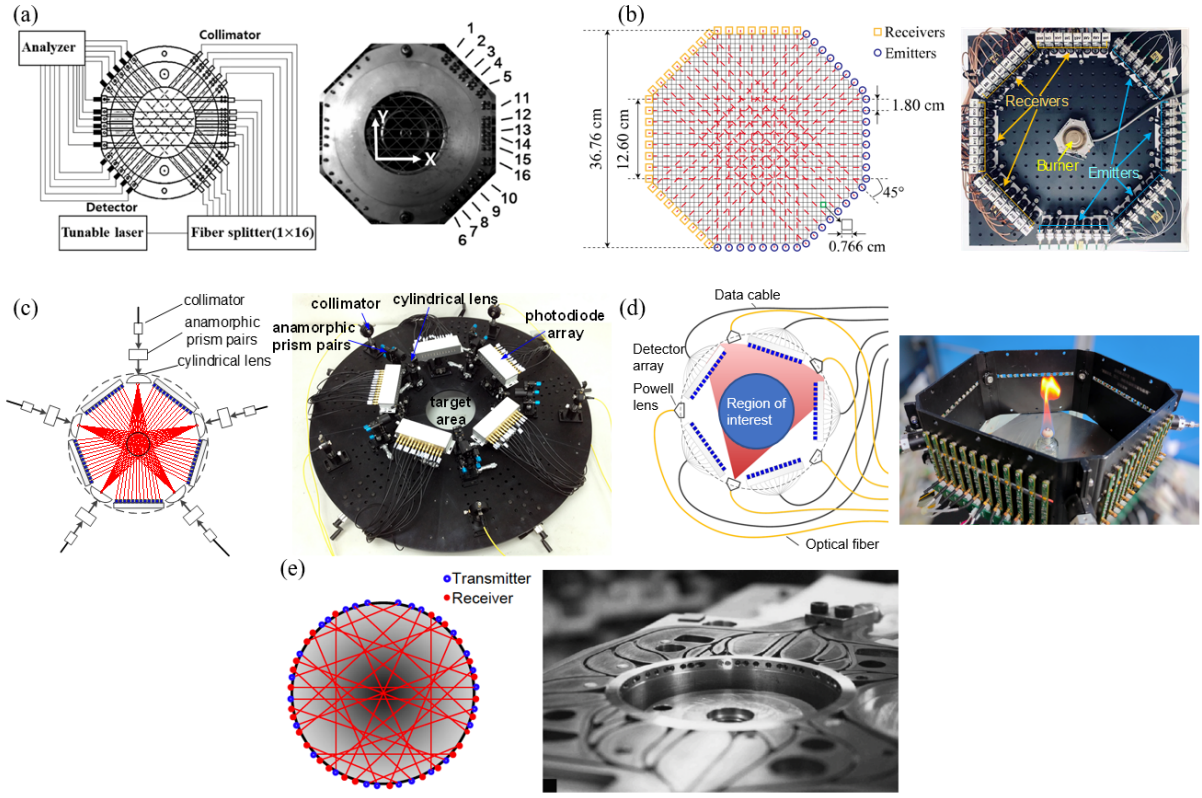

Fig. 3 Industrial applications of fixed-beam CST sensors on measurements of (a) power plant and combustion engine exhaust using a 3-view parallel-beam layout [57], (b) propane flames using a 4-view parallel beam layout [15], (c) swirl flames using fan-beam layouts [52, 58, 60], (d) wind tunnel using an angle-expanded fan-beam layout [51, 59], and (e) multi-cylinder automotive engine using an irregular-beam layout [47]. In each case, a schematic diagram of the CST sensor is shown on the left, and a photo of the fabricated sensor is shown on the right. Reprinted from [57] with permission from Creative Commons Attribution (CC BY 4.0). Adapted from [51, 52, 59] with permission from IEEE and Copyright Clearance Center. Reprinted with permission from [58] © The Optical Society. Reprinted from [60] with permission from AIP and Copyright Clearance Center. Adapted from [47] with permission from Elsevier and Copyright Clearance Center.

Generally speaking, a fixed-beam CST sensor is a duplication of multiple LOS LAS measurements according to the pre-determined beam arrangement. More LOS LAS measurements for angular (more than three projection angles) and linear sampling in the region of interest (ROI) definitely contribute to improved quality of the tomographic images. However, the resulting high complexity of optics design on, for example, laser emitters, receivers, light amplification and distribution systems, imposes significant challenges on the real-world implementation of CST. The potentially very high cost of the optics also hinders tomographic access for many researchers and process engineers. In principle, the optimal beam arrangement for a given application can be fundamentally determined by the requirement placed on the spatial resolution of the tomographic image. It can be envisaged that many fewer spatial samples are required for reconstructing a spatially smooth flame, e.g., a flat flame, than would be

required for a highly structure-detailed turbulence case. Based on the pioneering work on quantification of the spatial resolution of CST [17], customisation of the beam arrangement has been introduced for cost-effective design of fixed-beam CST sensors [18]. Given a certain number of laser beams, this customisation also helps in maximising the achievable spatial resolution of CST. Apart from the beam arrangement, statistical *a priori* information of the target field can further quantify the lower limit of the spatial resolution [19]. This mathematically-valid criterion can also be employed in the concept phase of the design of fixed-beam CST sensors.

Light delivery is also a technical challenge in the design of very large-size fixed-beam CST sensors, for example, with dimensions up to a few meters, which are required in practice for diagnosis of full-size industrial combustors. Most recently, a 126-beam CST sensor with 7-meter diameter has been designed and applied for imaging of a civil aero gas turbine exhaust with approx. 1.4-meter diameter [55]. The sensor has 6 projection angles, each with 21 laser beams. As shown in Fig. 4, neighbouring beams in the same projection are emitted in opposite directions to eliminate their crosstalk when received by the photodetectors. When designing, constructing and installing such a large-size sensor, the structural rigidity should be carefully modelled to suppress the point error caused by beam misalignment [61]. In addition, a distributed data acquisition system is required, to digitise the transmission signals at the front end and then transfer the digitised data to the back-end processors, in order to avoid the ambient noise that could be introduced by long-distance (~ 70 metre) transmission of analogue signals. More details of the electronics design will be introduced in Section 3.

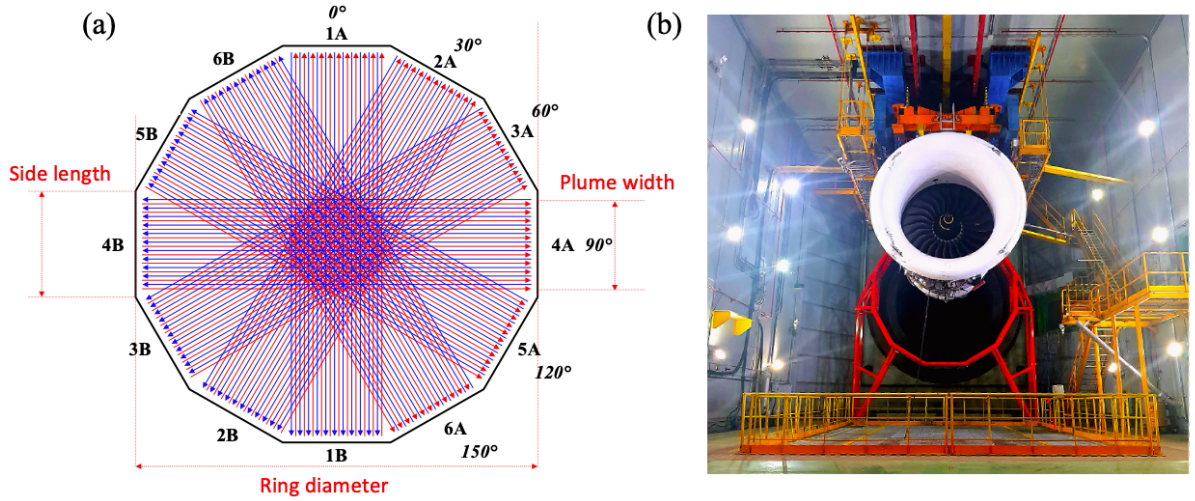

Fig. 4 Application of a 7-meter-diameter CST sensor on imaging of a civil aero gas turbine exhaust [55]. (a) Schematic diagram of the optical layout. (b) Picture of the CST sensor installed in a gas turbine test cell. Reprinted with permission from [55] © The Optical Society.

To date, 2D fixed-beam CST sensors are capable of reconstructing the specified cross-sectional distributions of flow parameters, at the expense of losing the out-of-plane imaging capability for characterisation of the spatial evolution of the flow. To reveal the inherently 3D nature of reactive flows, 3D fixed-beam CST will be required in the near future with moderate/high temporal response for instantaneous 3D imaging. Although several attempts have been made by using the scan-beam strategy for 3D imaging, the reconstruction, as noted above in Section 2.1, is only an indication of temporally and spatially averaged flows, and therefore, is less capable of characterising the kinetics of the target reactive flow fields. Further research may introduce multiple IR cameras for instantaneous 3D imaging. These cameras, as well as the pixels on each camera, need to be highly synchronised to simultaneously capture the 2D projections from multiple projection angles. However, the very high cost of the IR cameras, rigidness of the optical setup and limitations on the dimensions of the focal-plane array still present challenges for their industrial implementation.

The optical access of fixed-beam CST sensors to the process vessel at elevated pressure/temperature may also be addressed for next-generation optics development. To access flames under industry-relevant working conditions, pilot/large-scale combustion rigs commonly enclose the flames in steel or glass tubes, imposing significant challenges on the laser delivery to probe the in-combustor flames. Quartz and CaF_2 windows, with wedged surfaces to mitigate optical interference, have been used for LOS LAS measurements at NIR [62-64] and MIR wavelengths [65-67], respectively. However, layout of multiple laser beams at different projection angles is not only space-limited, but may also suffer from interference by window-introduced etalon effects. In comparison with open-path laser delivery, fibre optic technology provides better flexibility in these scenarios. Single-mode and multi-mode fibres have been employed for NIR laser delivery in CST systems applied to automotive engines for in-cylinder [47, 48] and exhaust [50] imaging. In case of closed combustion systems where windows are unavoidable, the fibre-coupled emitting and receiving ends can be arrangement much closer to the windows compared to the open-path solution. This implementation will facilitate the removal of ambient absorption in practical testing environments. More modelling, simulation and experiments are needed for MIR laser delivery. Hollow-core fibres have been demonstrated for laser coupling and delivery at MIR wavelengths [68-70]. However, they still suffer from several technical challenges in their application to MIR CST sensors, for example, the inadequate coupling efficiency, high attenuation for long-distance propagation and ease of damage in harsh environments. With the above challenges addressed and field tests carried out, hollow-core fibres could become promising candidates for multi-beam MIR laser delivery to implement fixed-beam CST sensors.

3 Electronics

The electronics of a CST system mainly consist of circuits for laser driving, photodiode signal conditioning and processing, and data acquisition (DAQ). To date, the laser driving circuits are commercially available for precise control, via temperature/current tuning, of the laser wavelength and intensity. The photodiode detectors (PDs) are used to convert the optical signal to a current signal, which is trans-impedance amplified (TIA), in either a single-ended or differential manner [71], to a certain level of voltage to facilitate the subsequent DAQ. In comparison, the most challenging electronics of a CST system is the DAQ. In this section, we will first give an overview of the DAQ electronics and introduce its basic elements. Then, we will introduce the principles of two representative state-of-the-art DAQ schemes, address the benefits and limitations of each scheme, and highlight their existing applications.

CST DAQ generally involves three sequential stages: (a) conditioning of the TIA signal, (b) digitising the conditioned signal, and (c) transferring/storing the digitised signal. Fig. 5 demonstrates the flow diagram of a general-purpose N-beam CST DAQ system. Each incident laser beam with intensity $I_{0,i}$ (i = 1, 2, … N) penetrates the absorbing gas sample, resulting in a transmitted laser intensity $I_{t,i}$ (i = 1, 2, … N). The specifications of the DAQ system depend on the techniques that implement the LAS measurement, in the state-of-the-art quoted literatures [2, 72, 73], using either Direct Absorption Spectroscopy (DAS) or Wavelength Modulation Spectroscopy (WMS).

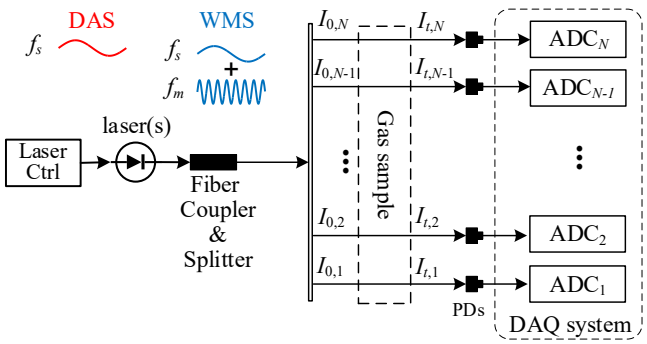

Fig. 5 Flow diagram of a general-purpose fully parallel CST DAQ system.

DAS can be used in two ways for CST: with a fixed wavelength tuned at the absorption wavelength of the target species; or by carrying out a wavelength-scan to tune through all or part of an absorption feature of the target species. The fixed-wavelength approach requires that attenuation of the beams by mechanisms other than spectroscopic absorption by the target species, e.g., due to refractive index variations within the ROI, is taken into account, and that the temperature- and pressure-dependence of absorption at the fixed wavelength is known. In favourable circumstances, e.g., imaging of the distribution of relatively large molecules with broad spectral features, the fixed-wavelength approach can readily achieve very high imaging speeds, up to 4,000 fps for in-cylinder imaging of automotive fuels gasoline, with typically 8 carbon atoms per target molecule [9, 23, 47], and diesel, with typically 12 carbon atoms per target molecule [49]. Over the last decade, however, the overwhelming majority of attention has been focused on molecules containing typically 2 or 3 atoms in total, with much narrower spectral features, requiring very delicate accounting for temperature- and pressure-dependence. For that reason, the fixed-wavelength approach is not discussed further in the text below.

To use the wavelength-scan DAS measurement method for CST, a ramp or sinusoidal wavelength scan signal is imposed on the laser diode. The resulting TIA signal generally needs to be conditioned by a low-pass filter and/or a second-stage amplification to fit with the input range of the analogue-to-digital converter (ADC) [60]. In general, the frequency of the wavelength scan is from several Hz to tens of kHz for commercial-off-the-shelf distributed feedback (DFB) laser diodes, requiring a sampling rate of the DAQ up to a few Mega Samples per second (MSps). For a CST system with tens of laser beams, as an example, the fully parallel DAQ data throughput is generally less than 1 Gbps, which can be streamed in real time by Ethernet. To date, DAS-based CST DAQ systems have been developed for monitoring low-turbulence flows, for example, laminar flames generated by flat flame burners and Bunsen burners [60, 74-76], and diesel engine exhaust [25, 77]. Commercial off-the-shelf DAQ systems, such as National Instruments DAQs (see www.ni.com), are also available to satisfy the requirement of DAS-based CST measurement. It is noteworthy that recent advances in MHz-rate scanned DAS were achieved to capture the highly transient reactions occurring at microsecond timescales [67, 78-82]. Although no attempt has been made to achieve CST using such a scan rate, it is a potential solution to further improve the temporal resolution of CST and will be discussed later in Section 4.2.

In industrial environments, line-of-sight LAS measurements are contaminated by noise from many sources, such as optical noise from beam steering caused by turbulence or thermal gradients, electronic noise from the DAQ hardware, and environmental noise from mechanical vibration [83-85]. To achieve stronger noise rejection performance, the WMS technique has been widely used in industrial CST. Typically, WMS is implemented by driving a laser diode with a low-frequency wavelength-scan signal, f_s (several Hz to a few kHz), with a small-amplitude high-frequency modulation signal, f_m, (tens of kHz to hundreds of kHz) superimposed upon it [72]. Given f_m of 100 kHz, for example, a reasonable sampling rate of 20 MSps for 16-bit digitization of the n^{th}-order WMS harmonics at $n \times f_m$ ($n \geq 2$) yields a single-channel data rate of 320 Mbit/s. For the same CST system with tens of laser beams as above, the overall data throughput is >10 Gbps. This can overload the real-time data communication between the front-end DAQs and the back-end high-level processors. Commercial high-speed and multi-channel PXI(e) DAQ systems may be used for fast in-memory data storage. However, it will easily overflow the memory in a few seconds of measurement. Therefore, the DAQ system should be designed with data throughput manageable for data communication and storage.

In the following, we will introduce two state-of-the-art DAQ schemes, time-division-multiplexing (TDM) and system-on-chip signal processing (SoC-SP), to reduce the data throughput for fast and continuous WMS-based CST measurement. We will demonstrate the implementation of each scheme, from the perspectives of hardware and/or firmware design, and introduce their suitability and potential limitations in industrial CST.

3.1 TDM DAQ schemes

TDM DAQ schemes are implemented by multiplexing the signals from the detected laser beams, referred to hereinafter as "measurement channels", either between successive wavelength scans (inter-scan TDM) or between successive modulation periods (in-scan TDM). Since the load on data communication is only occupied by the selected channel(s), TDM DAQ schemes reduce the data throughput of CST and the bandwidth compared to the fully parallel DAQ scheme. Moreover, such schemes simplify the hardware, in which only one or a few ADCs are needed to digitise all the CST measurement channels.

The inter-scan TDM can be implemented at a sampling interval of $1/(2f_s)$ for a given sinusoidal scan, as shown in Fig. 6. The laser transmission signal, $I_{t,i}$, from the i-th selected measurement channel is digitised by the ADC, then streamed to and stored in the high-level workstation for post-processing of the harmonics. Consequently, the sampled data is a sequential connection of the multi-channel signal. However, such a scheme degrades the CST temporal resolution. A single frame of image can only be reconstructed after all the CST measurement channels are multiplexed, resulting in the CST temporal resolution of $2f_s/N$ fps. Here, N denotes the number of multiplexed channels. Given a sinusoidal scan with $N = 2$, the temporal resolution of the inter-scan TDM DAQ is f_s fps. However, the sampling interval between the neighbouring measurement channels is determined by f_s, and is at millisecond to sub-second level given f_s in the range several Hz to a few kHz. In the case of turbulent reactive-flow monitoring, such a sampling interval leads to asynchronous measurement of the multiple laser beams, which may be insufficient for characterising the instantaneous thermophysical and chemical reactions.

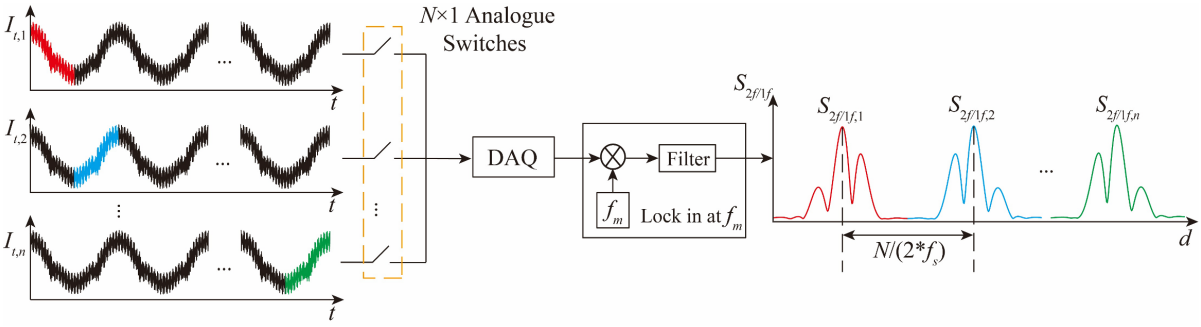

Fig. 6. Flow diagram of the inter-scan TDM DAQ scheme for CST at a sampling interval of $1/2f_s$ with sinusoidal scan.

To improve synchrony of multi-channel CST sampling, the in-scan TDM DAQ scheme was recently proposed with the same hardware complexity as the TDM implementation [86]. As shown in Fig. 7, this scheme is achieved by multiplexing the multi-channel signals over the high-frequency modulation within a wavelength scan. Consequently, the CST temporal resolution achieved by the in-scan TDM DAQ is f_s fps, which is the same as that achieved by a fully parallel DAQ. Since the neighbouring-channel sampling interval achieved by the in-scan TDM scheme is reduced to $1/f_m$ (microsecond-level), this scheme is also named as quasi-parallel (QP) DAQ to emphasise its near-equivalence to fully parallel DAQ [87]. However, the implementation of the in-scan TDM generally requires a high modulation-to-scan frequency ratio (f_m/f_s). In the WMS technique, the spectral resolution of the extracted harmonics depends on the density of wavelength modulation within a wavelength scan. When using the in-scan TDM, the modulation periods within a wavelength scan are equally shared by the multiplexed channels, resulting in worsened spectral resolution in each channel. For example, given maximal f_m of 300 kHz with adequate modulation depth and acceptable nonlinearity, f_s of 1 kHz could maximally give a total of 300 modulation periods within a ramp scan. In case of multiplexing among 4 measurement channels, there are only 75 modulation periods sampled by each channel, which is insufficient for maintaining spectral integrity for CST measurement with adequate SNRs. These fundamentals limit the scan frequency and thus the imaging rate up to a few hundred Hz.

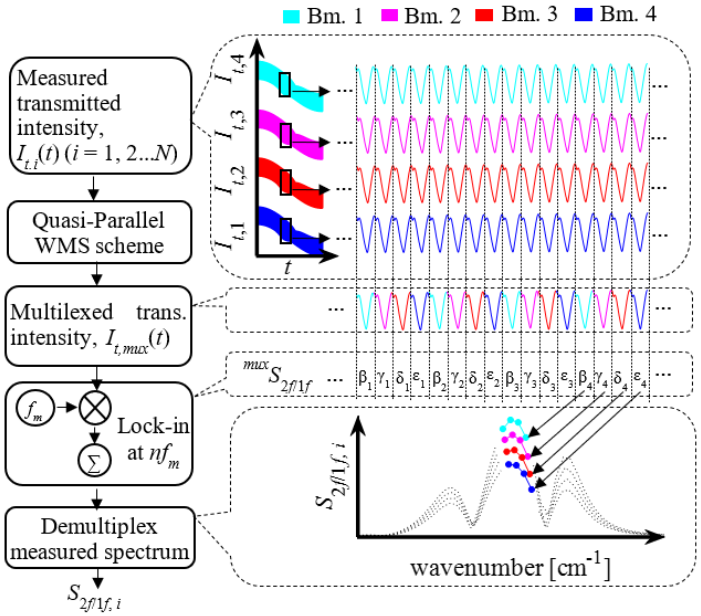

Fig. 7. Flow diagram of the in-scan TDM DAQ scheme for CST [86]. Adapted from [86] with permission from IEEE and Copyright Clearance Center.

3.2 SoC-SP DAQ schemes

In the last decade, SoC-SP schemes have been emerging to achieve high-speed CST measurement. These schemes firstly implement digital lock-in (DLI) [72], mostly on a field programmable gate array (FPGA) and/or a digital signal processor (DSP), to obtain the in-phase (I) and quadrature (Q) components of the n^{th}-order harmonics of the laser transmission. The I and Q components are also processed by the SoC, with the important features extracted and fed as projection data for image reconstruction. Fig. 8 shows three state-of-the-art SoC-SP methods developed for WMS-based CST DAQ. The most simplified features are the peak values of the harmonics [59, 88-90] shown in Fig. 8(a), which can be used for calibration-free WMS measurement. However, the extracted peaks can be easily disturbed by measurement noise since they are unable to indicate the absorbance lineshape, which is a chemo-physical filter in WMS for noise rejection. To maintain sufficient information of the spectral lineshape, quadrature demodulation methods have been introduced and implemented by SoC for WMS-based CST DAQ systems, as shown in Fig. 8(a). These methods include classic whole-modulation-period demodulation [87, 91], Kalman filter-based recursive demodulation [92] and cascaded integrator-comb (CIC) filter-based demodulation [93, 94]. The demodulation methods reduce data throughput, enabling uninterrupted communication between the DAQ system and the high-level processors. Most recently, neural networks are deployed within the SoC to extract spectral features, such as the peaks of the harmonics or the path-integrated absorbances shown in Fig. 8(c) [92, 95]. The neural networks enable very fast computation, which facilitates real-time WMS measurement and image visualisation. However, great care needs to be taken in the training process by integrating real-world noises, optical interferences and laser characteristics into the training network. In addition, signal pre-processing, such as normalisation of the beam-dependent incident laser intensity, may be needed for the training process. Each laser beam may need to be trained individually by taking the beam-dependent parameters, such as intensity-wavelength phase dependences, into account. Consequently, a parameter-specific neural network is needed for each line-of-sight WMS measurement. For a multi-beam CST system, all the neural networks to be deployed could possibly exceed the available resources of the SoCs.

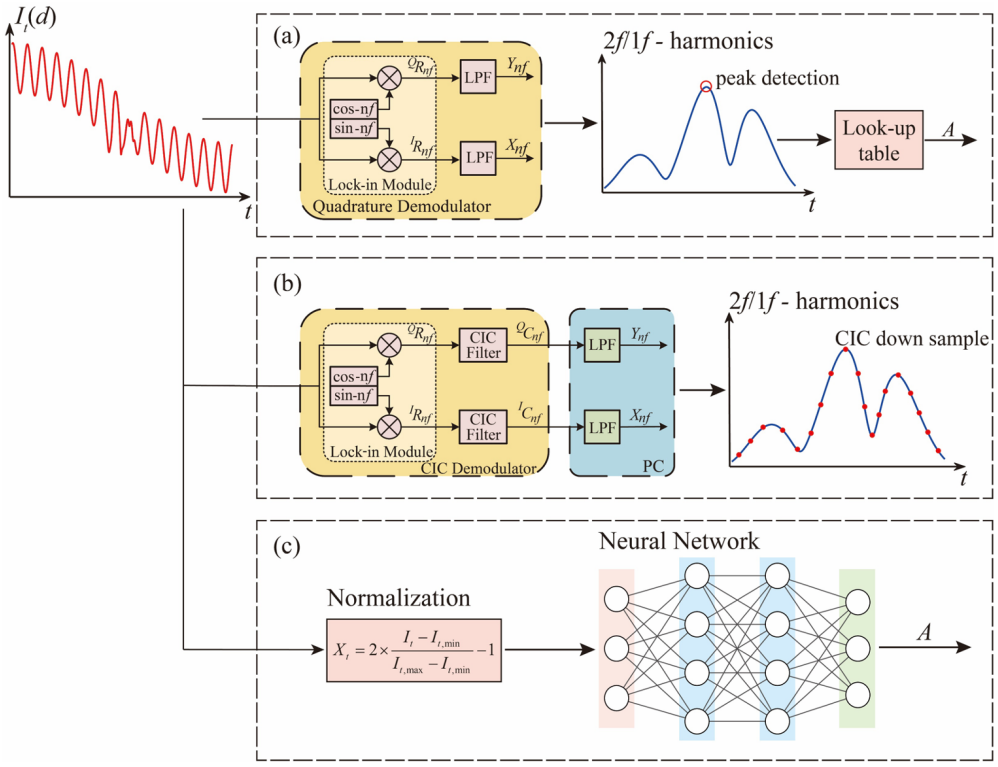

Fig. 8. Three state-of-the-art SoC-SP methods, (a) harmonic peak extraction [88], (b) spectra-maintained CIC-filter assisted demodulation [93], and (c) neural network [92] for WMS-based CST DAQ.

In pilot-scale and large-scale industrial applications of CST, the optical sensors need to be located close to the DAQ systems, typically within a few tens of centimetres. This implementation can digitise the multi-channel TIA signals locally, enabling long-distance transfer of the digitised signal with good SNRs. Therefore, a distributed DAQ system is required in practice, in which a star topology [96] can be used to connect all the DAQ hubs to the high-level processor. Each DAQ hub samples the TIA signals from the assigned laser beams. All the DAQ hubs must be strictly synchronised to avoid phase shift of the harmonics between the hubs and between the measurement channels on each hub. To date, a distributed DAQ system has been designed for implementing CST on the exhaust plume of aero-engines using 126 laser beams [87]. Further improvement can be considered on the reconfigurability of the distributed DAQ system. When applied to CST sensors with more laser beams, the DAQ channels can be flexibly extended without major modification of the hardware electronics.

4 Further improvements on spatiotemporal resolution

Apart from the above-mentioned hardware development of optics and electronics, the spatiotemporal resolution of CST can be further improved by introducing more physical information and faster laser driving schemes, respectively. In this section, we will briefly introduce these improvements, address their instrumental challenges and point out a potential way forward.

4.1 Spatial resolution – Enrich the image reconstruction with physical flow-field information

Geometrically, spatial resolution of CST can be improved by arranging more projection angles and more laser beams per angle (see Section 2). When the miniaturisation of the optics and opto-mechanics to achieve denser beam coverage reaches the limit, physically informed *a priori* information can be utilised to further improve the spatial resolution. Since the inverse problem of CST is rank-deficient, incorporation of *a priori* information into the tomographic algorithm can reduce the degrees of freedom in the retrieval and thus improve the image quality [22]. Typical *a priori* information includes the physical assumption of smooth distributions and non-negativity of the flow-field parameters [3, 97]. A

simplified form of penalisation between the accuracy and robustness of the solution has also been imposed using regularisation methods. These implicit assumptions perform as “low-pass filters”, which suppress the artefacts introduced by rank deficiency in the image reconstruction, but inevitably blur the real structural details of the target flow. This over-filtering effect will particularly damage the reconstruction of hydrodynamic features in turbulent flows. Motivated by aggregate reconstruction accuracy properties, a Bayesian framework using explicit likelihood and prior probability density functions has been proposed to improve the CST imaging fidelity [12, 98, 99]. Implied in the above Bayesian formulation, Bayesian model selection has been introduced to select the optimal mesh density, model of interpolation and *a priori* information, providing superior trade-off between parameter uncertainty and model error.

Recently, the physical information of fluid dynamics has been integrated into deep neural networks to predict the distributions of gas parameters in reactive flows. Examples of this approach have been attempted by deriving the physical information from Large Eddy Simulation (LES). The LES results were used to train end-to-end neural networks, which directly reconstruct the absorption fields from the CST measurements [100, 101]. These attempts indeed allow for incorporation of thermochemistry and flow-field transport models into image reconstruction. However, predictive capability of these neural networks fully depends on the simulation-generated training sets. In practice, the neural networks could be invalid if the hydrodynamic features of the experimental flow fields are different from the simulated ones. Further efforts have been made by incorporating the governing physics, such as the simplified Navier–Stokes and advection–diffusion equations, and the projection model, into the network training process [16, 102]. These physics-informed neural networks (PINNs) improve generalisation ability and accuracy in the presence of measurement noise. However, the PINNs could also suffer uncertainties when the physics prior is less predictable in the reactive flow, such as combustion processes, in which the complex equations of heat transfer and chemical kinetics need to be additionally embedded. Overall, discrepancies between the training models and the real-world scenarios are the limitation of “direct” reconstruction of the flow-field parameters from limited CST measurements. Instead, researchers could consider “indirect” and “less ambitious” learning of the hydrodynamic features. For example, gradients of the data discrepancy can be learned iteratively by making use of spatial and temporal variances of the hydrodynamic features. Physically meaningful noise models [83, 84], including laser noise, detector noise, ADC noise, optical noise and environmental noise, need to be integrated into the training model. Preferably, the noise models should be quantified from real experiments and in real working conditions to improve the generalisation of the neural networks.

4.2 Temporal resolution - Freeze the image reconstruction with faster laser driving schemes

As described in Sections 2 and 3, the combination of a fixed-beam CST sensor and a fully parallel DAQ system maximises the temporal resolution of a CST imaging system. Since the speed of wavelength scanning determines the repetition rate of the CST measurement, i.e., the temporal resolution, the agility of laser driving sets the upper limit of the temporal resolution. In the extreme case, the fastest laser driving scheme enables the reconstruction of each individual image in a frozen time scale, contributing to the penetration of highly transient processes, such as supersonic/hypersonic propulsion, detonations and explosions.

Faster laser driving schemes can be achieved by rapid wavelength sweeping of individual laser diodes. For example, faster scan signals (near MHz) and modulation signals (35 to 45 MHz) have been used for high-speed line-of-sight DAS and WMS measurement [67, 78-82, 103]. Assisted by bias-tee circuitry, diplexed radio frequency (RF) wavelength scan signals were imposed on continuous-wave distributed-feedback QCLs to measure line-of-sight thermodynamic and thermochemical properties at MHz rates [79-82]. When imposing long pulses on the QCLs, the down-chirp induced intrapulse spectra have been used for rapid sensing of temperature and species concentration [104-107]. The pulse repetition rates reported in the literature are generally limited to a few hundred kHz, due to spectral

distortion at higher rates. In addition, the laser diodes can be driven by short pulse signals, which can cause quantised rotational excitation of target molecules. The excited molecules will initially rotate in phase with each other and radiate coherently to emit a forward burst of radiation, referred to as free induction decay (FID) or a modified form of the FID (m-FID) signals [108]. The m-FID signals, generated from cepstral analysis of the time-domain transmission signal, can be used for high-accuracy and high-speed absorption spectroscopic measurement [108-110].

Alternatively, frequency-agile laser sources, such as Fourier domain mode-locking lasers [111-113] and supercontinuum lasers [114-118], can be utilised to rapidly and continuously scan the laser wavelength across a wide range of absorption spectra. For example, tens of nanometres in wavelength can be scanned within tens of nanoseconds (ns) to a few microseconds (μs), resulting in MHz-rate temporal resolution. The enriched broad-bandwidth spectral information also enables access to more transitions and the absorption lineshapes between the neighbouring transitions [3, 119-122]. This will substantially benefit CST measurement at elevated pressures since the broadening effects on the absorption spectra can be adequately covered.

To implement the two schemes mentioned above, the requirements of expensive GHz-bandwidth TIA and GSps-digitisation DAQ are placed on each LAS measurement channel. When populating to multi-channel CST, the massive data amount and data throughput impose significant challenges on the speed of real-time signal processing (even with the most modern high-level processors) and communication (even with the highest speed communication protocols). By high-speed streaming the data to the built-in but size-limited memory, these schemes are more appropriate to capture a very short period, e.g., tens to hundreds of μs, of the highly transient processes.

5 Summary and outlook

It is clear that CST instrumentation is becoming increasingly sophisticated for imaging thermophysical and thermochemical parameters in reactive flows. New optics and electronics have been designed in the past decade and will continue to emerge in the energy-generation industries, for example, to validate numerical combustion models, analyse transient combustion processes, monitor carbon and pollutant emissions, and inform the effectiveness of sustainable fuels and novel combustor architectures.

On the optics side, light delivery schemes and technologies still need to be improved with greater effectiveness to finely resolve the detailed flow-field features in small-scale sensing applications, and with great robustness to survive the harsh environments in large-scale and industrial application. Projecting CST optics into the future, CST at MIR sensing wavelengths, which has been barely investigated to date due to the lack of reliable and effective MIR light delivery, will be further developed for more sensitive imaging of trace gaseous components. Furthermore, optical sensors are expected to break through the existing 2D barrier for instantaneous imaging, to unveil the 3D nature of the turbulent flows with 3D instantaneous imaging.

On the electronics side, research in high-bandwidth DAQs and high-speed SoC-SP techniques will continue to improve the speed of CST imaging. Existing challenges on high data throughput are yet to be overcome in the case of measuring hundreds of laser beams and/or at kilo fps-level frame rates. Accompanied by the rapid development of AI-driven hardware, machine/deep learning approaches have shown potential to speed up SoC signal processing, but must carefully integrate the analytically tomographic model and experimental data into the network training.

Though exciting instrumentation advances are on the horizon, the main challenges remain on improving the spatiotemporal resolution of CST imaging. We expect new interdisciplinary opportunities to arise from rapid progress in the communities of optical engineering, electronic engineering, mechanical engineering and data science, which will fill in the research gaps that limit the spatiotemporal resolution from the perspectives of laser technology, hardware-acceleration technology, CFD technology, and

data-driven technology, respectively. Finally, it is noteworthy that CST is fundamentally preferable for gas-phase diagnostics. To inform the multi-physics and multi-phase nature of reactive flows, fusion of CST and other active/passive optical imaging techniques, e.g., laser induced incandescence (LII), particle image velocimetry (PIV), planar/volumetric laser induced fluorescence (P/V-LIF) and volumetric emission tomography, remains to be explored in the near future.

Data availability statement

No new data were created or analysed in this study.

Acknowledgments

The authors are also grateful for the EPSRC Programme Grant *LITECS* (EP/T012595/1), EPSRC Platform Grant *CIDER* (EP/P001661/1), EU H2020 Cleansky 2 Project *CIDAR* (JTI-CS2-2017-CFP06-ENG-03-16) and NSFC Grants (61827802, U2241259), that supported the writing of this article.

References

[1] H. McCann, P. Wright, K. Daun *et al.*, "5 - Chemical Species Tomography," *Industrial Tomography (Second Edition)*, M. Wang, ed., pp. 155-205: Woodhead Publishing, 2022.

[2] C. Liu, and L. Xu, "Laser absorption spectroscopy for combustion diagnosis in reactive flows: A review," *Applied Spectroscopy Reviews,* vol. 54, no. 1, pp. 1-44, 2019.

[3] W. Cai, and C. F. Kaminski, "Tomographic absorption spectroscopy for the study of gas dynamics and reactive flows," *Progress in Energy and Combustion Science,* vol. 59, pp. 1-31, 2017.

[4] B. Halls, P. Hsu, S. Roy *et al.*, "Two-color volumetric laser-induced fluorescence for 3D OH and temperature fields in turbulent reacting flows," *Opt. Lett.,* vol. 43, pp. 2961-2964 2018.

[5] L. Ma, Q. Lei, T. Capil *et al.*, "Direct comparison of two-dimensional and three-dimensional laser-induced fluorescence measurements on highly turbulent flames," *Optics Letters,* vol. 42, no. 2, pp. 267-270, 2017.

[6] S. J. Grauer, K. Mohri, T. Yu *et al.*, "Volumetric emission tomography for combustion processes," *Progress in Energy and Combustion Science,* vol. 94, pp. 101024, 2023.

[7] K. Mohri, S. Görs, J. Schöler *et al.*, "Instantaneous 3D imaging of highly turbulent flames using computed tomography of chemiluminescence," *Applied Optics,* vol. 56, no. 26, pp. 7385-7395, 2017.

[8] S. Scharnowski, and C. J. Kähler, "Particle image velocimetry - Classical operating rules from today's perspective," *Optics and Lasers in Engineering,* vol. 135, pp. 106185, 2020.

[9] F. P. Hindle, S. J. Carey, K. Ozanyan *et al.*, "Measurement of gaseous hydrocarbon distribution by a near-infrared absorption tomography system," *Journal of Electronic Imaging,* vol. 10, no. 3, pp. 593-600, 2001.

[10] T. Yu, and W. Cai, "Benchmark evaluation of inversion algorithms for tomographic absorption spectroscopy," *Applied Optics,* vol. 56, no. 8, pp. 2183-2194, 2017.

[11] Y. Bao, R. Zhang, G. Enemali *et al.*, "Relative Entropy Regularized TDLAS Tomography for Robust Temperature Imaging," *IEEE Transactions on Instrumentation and Measurement,* vol. 70, pp. 1-9, 2021.

[12] S. J. Grauer, P. J. Hadwin, and K. J. Daun, "Bayesian approach to the design of chemical species tomography experiments," *Applied Optics,* vol. 55, no. 21, pp. 5772-5782, 2016.

[13] W. Cai, D. J. Ewing, and L. Ma, "Investigation of temperature parallel simulated annealing for optimizing continuous functions with application to hyperspectral tomography," *Applied Mathematics and Computation,* vol. 217, no. 12, pp. 5754-5767, 2011.

[14] J. Huang, H. Liu, J. Dai *et al.*, "Reconstruction for limited-data nonlinear tomographic absorption spectroscopy via deep learning," *Journal of Quantitative Spectroscopy and Radiative Transfer,* vol. 218, pp. 187-193, 2018.

[15] Y. Jiang, J. Si, R. Zhang *et al.*, "CSTNet: A Dual-Branch Convolutional Neural Network for Imaging of Reactive Flows Using Chemical Species Tomography," *IEEE Transactions on Neural Networks and Learning Systems*, 2022.

[16] J. P. Molnar, and S. J. Grauer, "Flow field tomography with uncertainty quantification using a Bayesian physics-informed neural network," *Measurement Science and Technology,* vol. 33, no. 6, pp. 065305, 2022.
[17] S. A. Tsekenis, N. Tait, and H. McCann, "Spatially resolved and observer-free experimental quantification of spatial resolution in tomographic images," *Review of Scientific Instruments,* vol. 86, no. 3, pp. 035104, 2015.
[18] C. Liu, S. Tsekenis, N. Polydorides *et al.*, "Toward Customized Spatial Resolution in TDLAS Tomography," *IEEE Sensors Journal,* vol. 19, no. 5, pp. 1748-1755, 2019.
[19] J. Emmert, S. Wagner, and K. J. Daun, "Quantifying the spatial resolution of the maximum a posteriori estimate in linear, rank-deficient, Bayesian hard field tomography," *Measurement Science and Technology,* vol. 32, no. 2, pp. 025403, 2020.
[20] C. Ruan, F. Chen, W. Cai *et al.*, "Principles of non-intrusive diagnostic techniques and their applications for fundamental studies of combustion instabilities in gas turbine combustors: A brief review," *Aerospace Science and Technology,* vol. 84, pp. 585-603, 2019.
[21] M. Aldén, J. Bood, Z. Li *et al.*, "Visualization and understanding of combustion processes using spatially and temporally resolved laser diagnostic techniques," *Proceedings of the Combustion Institute,* vol. 33, no. 1, pp. 69-97, 2011.
[22] K. J. Daun, S. J. Grauer, and P. J. Hadwin, "Chemical species tomography of turbulent flows: Discrete ill-posed and rank deficient problems and the use of prior information," *Journal of Quantitative Spectroscopy and Radiative Transfer,* vol. 172, pp. 58-74, 2016.
[23] N. Terzija, J. L. Davidson, C. A. Garcia-Stewart *et al.*, "Image optimization for chemical species tomography with an irregular and sparse beam array," *Measurement Science & Technology,* vol. 19, no. 9, pp. 094007, 2008.
[24] J. Emmert, H. Schneider, B. Böhm *et al.*, "Phase-locked absorption tomography for retrieving 5 kHz time-resolved tracer profiles in solid fuel combustion," *Applications in Energy and Combustion Science,* vol. 12, pp. 100093, 2022.
[25] E. F. Nasir, and S. T. Sanders, "Laser absorption tomography for ammonia measurement in diesel engine exhaust," *Applied Physics B,* vol. 126, no. 11, pp. 178, 2020.
[26] J. Foo, and P. A. Martin, "Tomographic imaging of reacting flows in 3D by laser absorption spectroscopy," *Applied Physics B,* vol. 123, no. 5, pp. 160, 2017.
[27] L. Ma, K. Duan, K.-P. Cheong *et al.*, "Multispectral infrared absorption spectroscopy for quantitative temperature measurements in axisymmetric laminar premixed sooting flames," *Case Studies in Thermal Engineering,* vol. 28, pp. 101575, 2021.
[28] C. Wei, K. K. Schwarm, D. I. Pineda *et al.*, "Volumetric laser absorption imaging of temperature, CO and CO2 in laminar flames using 3D masked Tikhonov regularization," *Combustion and Flame,* vol. 224, pp. 239-247, 2021.
[29] X. Liu, G. Zhang, Y. Huang *et al.*, "Two-dimensional temperature and carbon dioxide concentration profiles in atmospheric laminar diffusion flames measured by mid-infrared direct absorption spectroscopy at 4.2 μm," *Applied Physics B,* vol. 124, no. 4, pp. 61, 2018.
[30] K.-P. Cheong, D. Shi, S. Liu *et al.*, "Tomographic Absorption Spectroscopy for H2O Transport in a Laminar Jet with Inverse Concentration Gradient," *Sensors,* 22, 2022].
[31] K.-P. Cheong, L. Ma, Z. Wang *et al.*, "Influence of Line Pair Selection on Flame Tomography Using Infrared Absorption Spectroscopy," *Applied Spectroscopy,* vol. 73, no. 5, pp. 529-539, 2018.
[32] X. Liu, G. Wang, J. Zheng *et al.*, "Temporally resolved two dimensional temperature field of acoustically excited swirling flames measured by mid-infrared direct absorption spectroscopy," *Optics Express,* vol. 26, no. 24, pp. 31983-31994, 2018.
[33] V. Kasyutich, and P. Martin, "Towards a two-dimensional concentration and temperature laser absorption tomography sensor system," *Applied Physics B: Lasers and Optics,* vol. 102, no. 1, pp. 149-162, 2011.
[34] S. A. Tsekenis, and N. Polydorides, "Optical access schemes for high speed and spatial resolution optical absorption tomography in energy engineering," *IEEE Sensors Journal,* vol. 17, no. 24, pp. 8072-8080, 2017.

[35] T. A. Sipkens, S. J. Grauer, A. M. Steinberg *et al.*, "New transform to project axisymmetric deflection fields along arbitrary rays," *Measurement Science and Technology,* vol. 33, no. 3, pp. 035201, 2022.
[36] L. Ma, K.-P. Cheong, M. Yang *et al.*, "On the Quantification of Boundary Layer Effects on Flame Temperature Measurements Using Line-of-sight Absorption Spectroscopy," *Combustion Science and Technology,* vol. 194, no. 16, pp. 3259-3276, 2022.
[37] D. Wen, L. Ma, and Y. Wang, "Effects of thermochemical non-uniformity on line-of-sight laser absorption thermometry in counterflow diffusion flames," *Journal of Quantitative Spectroscopy and Radiative Transfer,* vol. 277, pp. 107990, 2022.
[38] N. A. Malarich, and G. B. Rieker, "Resolving nonuniform temperature distributions with single-beam absorption spectroscopy. Part I: Theoretical capabilities and limitations," *Journal of Quantitative Spectroscopy and Radiative Transfer,* vol. 260, pp. 107455, 2021.
[39] N. A. Malarich, and G. B. Rieker, "Resolving nonuniform temperature distributions with single-beam absorption spectroscopy. Part II: Implementation from broadband spectra," *Journal of Quantitative Spectroscopy and Radiative Transfer,* vol. 272, pp. 107805, 2021.
[40] X. Liu, J. B. Jeffries, and R. K. Hanson, "Measurement of nonuniform temperature distributions using line-of-sight absorption spectroscopy," *AIAA J,* vol. 45, no. 2, pp. 411-419, 2007.
[41] C. S. Goldenstein, I. A. Schultz, J. B. Jeffries *et al.*, "Two-color absorption spectroscopy strategy for measuring the column density and path average temperature of the absorbing species in nonuniform gases," *Appl. Opt.,* vol. 52, no. 33, pp. 7950-7962, 2013.
[42] C. Liu, L. Xu, and Z. Cao, "Measurement of nonuniform temperature and concentration distributions by combining line-of-sight TDLAS with regularization methods," *Appl. Opt.,* vol. 52, no. 20, pp. 4827-4842, 2013.
[43] L. H. Ma, L. Y. Lau, and W. Ren, "Non-uniform temperature and species concentration measurements in a laminar flame using multi-band infrared absorption spectroscopy," *Applied Physics B,* vol. 123, no. 3, pp. 83, 2017.
[44] C. Wei, D. I. Pineda, L. Paxton *et al.*, "Mid-infrared laser absorption tomography for quantitative 2D thermochemistry measurements in premixed jet flames," *Applied Physics B,* vol. 124, no. 6, pp. 123, 2018.
[45] C. Wei, D. I. Pineda, C. S. Goldenstein *et al.*, "Tomographic laser absorption imaging of combustion species and temperature in the mid-wave infrared," *Optics Express,* vol. 26, no. 16, pp. 20944-20951, 2018.
[46] R. J. Tancin, R. M. Spearrin, and C. S. Goldenstein, "2D mid-infrared laser-absorption imaging for tomographic reconstruction of temperature and carbon monoxide in laminar flames," *Optics Express,* vol. 27, no. 10, pp. 14184-14198, 2019.
[47] P. Wright, N. Terzija, J. L. Davidson *et al.*, "High-speed chemical species tomography in a multi-cylinder automotive engine," *Chemical Engineering Journal,* vol. 158, no. 1, pp. 2-10, 2010.
[48] N. Terzija, S. Karagiannopoulos, S. Begg *et al.*, "Tomographic imaging of the liquid and vapour fuel distributions in a single-cylinder direct-injection gasoline engine," *International Journal of Engine Research,* vol. 16, no. 4, pp. 565-579, 2015.
[49] S.-A. Tsekenis, K. G. Ramaswamy, N. Tait *et al.*, "Chemical species tomographic imaging of the vapour fuel distribution in a compression-ignition engine," *International Journal of Engine Research,* vol. 19, no. 7, pp. 718–731, 2018.
[50] F. Stritzke, S. van der Kley, A. Feiling *et al.*, "Ammonia concentration distribution measurements in the exhaust of a heavy duty diesel engine based on limited data absorption tomography," *Optics Express,* vol. 25, no. 7, pp. 8180-8191, 2017.
[51] W. Zhao, L. Xu, A. Huang *et al.*, "A WMS based TDLAS tomographic system for distribution retrievals of both gas concentration and temperature in dynamic flames," *IEEE Sensors Journal,* vol. 20, no. 8, pp. 4179-4188, 2020.
[52] C. Liu, Z. Cao, Y. Lin *et al.*, "Online cross-sectional monitoring of a swirling flame using TDLAS tomography," *IEEE Transactions on Instrumentation and Measurement,* vol. 67, no. 6, pp. 1338-1348, 2018.

[53] Z. Wang, W. Zhou, J. Yan *et al.*, “Application of 2D temperature measurement to a coal-fired furnace using CT-TDLAS,” *Measurement Science and Technology,* vol. 31, no. 3, pp. 035203, 2019.
[54] Y. Deguchi, T. Kamimoto, Z. Z. Wang *et al.*, “Applications of laser diagnostics to thermal power plants and engines,” *Applied Thermal Engineering,* vol. 73, no. 2, pp. 1453-1464, 2014.
[55] A. Upadhyay, M. Lengden, G. Enemali *et al.*, “Tomographic imaging of carbon dioxide in the exhaust plume of largecommercial aero-engines,” *Applied Optics,* vol. 61, no. 28, pp. 8540-8552, 2022.
[56] D. McCormick, M. G. Twynstra, K. J. Daun *et al.*, "Optimising laser absorption tomography beam arrays for imaging chemical species in gas turbine engine exhaust plumes," *7th World Congress on Industrial Process Tomography*, 2013.
[57] M.-G. Jeon, D.-H. Doh, and Y. Deguchi, “Measurement Enhancement on Two-Dimensional Temperature Distribution of Methane-Air Premixed Flame Using SMART Algorithm in CT-TDLAS,” *Applied Sciences,* vol. 9, no. 22, 2019.
[58] C. Liu, L. Xu, J. Chen *et al.*, “Development of a fan-beam TDLAS-based tomographic sensor for rapid imaging of temperature and gas concentration,” *Opt. Express,* vol. 23, no. 17, pp. 22494-22511, 2015.
[59] M. Li, L. Xu, and Z. Cao, “TDLAS Tomography System for Online Imaging and Dynamic Process Playback of Temperature and Gas Mole Fraction,” *IEEE Transactions on Instrumentation and Measurement,* vol. 71, no. 2006210, pp. 1-10, 2022.
[60] L. Xu, C. Liu, W. Jing *et al.*, “Tunable diode laser absorption spectroscopy-based tomography system for on-line monitoring of two-dimensional distributions of temperature and H2O mole fraction,” *Review of Scientific Instruments,* vol. 87, no. 1, pp. 013101, 2016.
[61] P. Wright, D. McCormick, J. Kliment *et al.*, "Implementation of non-intrusive jet exhaust species distribution measurements within a test facility," *2016 IEEE Aerospace Conference.* pp. 1-14, 2016.
[62] G. C. Mathews, M. G. Blaisdell, A. I. Lemcherfi *et al.*, “High-bandwidth absorption-spectroscopy measurements of temperature, pressure, CO, and H2O in the annulus of a rotating detonation rocket engine,” *Applied Physics B,* vol. 127, no. 12, pp. 165, 2021.
[63] B. A. Dharmaputra, Y. Xiong, S. Shcherbanev *et al.*, "Entropy Waves Measurement by Tunable Diode Laser Absorption Spectroscopy," *AIAA SCITECH 2022 Forum*, AIAA SciTech Forum: American Institute of Aeronautics and Astronautics, 2021.
[64] W. Wei, W. Y. Peng, Y. Wang *et al.*, “Two-color frequency-multiplexed IMS technique for gas thermometry at elevated pressures,” *Applied Physics B,* vol. 126, no. 3, pp. 51, 2020.
[65] S. J. Cassady, W. Y. Peng, C. L. Strand *et al.*, “Time-resolved, single-ended laser absorption thermometry and H2O, CO2, and CO speciation in a H2/C2H4-fueled rotating detonation engine,” *Proceedings of the Combustion Institute,* vol. 38, no. 1, pp. 1719-1727, 2021.
[66] F. A. Bendana, D. D. Lee, S. A. Schumaker *et al.*, “Cross-band infrared laser absorption of carbon monoxide for thermometry and species sensing in high-pressure rocket flows,” *Applied Physics B,* vol. 125, no. 11, pp. 204, 2019.
[67] G. C. Mathews, M. Gomez, C. J. Schwartz *et al.*, “Experimental and synthetic laser-absorption-spectroscopy measurements of temperature, pressure, and CO at 1 MHz for evaluation of post-detonation fireball models,” *Proceedings of the Combustion Institute*, 2022.
[68] Z. Wang, H. Zhang, J. Wang *et al.*, “Photothermal multi-species detection in a hollow-core fiber with frequency-division multiplexing,” *Sensors and Actuators B: Chemical,* vol. 369, pp. 132333, 2022.
[69] P. Patimisco, V. Spagnolo, M. S. Vitiello *et al.*, “Low-Loss Hollow Waveguide Fibers for Mid-Infrared Quantum Cascade Laser Sensing Applications,” *Sensors (Basel, Switzerland),* vol. 13, no. 1, pp. 1329-1340, 2013.
[70] J. Li, S. Yang, Z. Du *et al.*, “Quantitative analysis of ammonia adsorption in Ag/AgI-coated hollow waveguide by mid-infrared laser absorption spectroscopy,” *Optics and Lasers in Engineering,* vol. 121, pp. 80-86, 2019.
[71] P. Wright, K. B. Ozanyan, S. J. Carey *et al.*, “Design of high-performance photodiode receivers for optical tomography,” *Sensors Journal, IEEE,* vol. 5, no. 2, pp. 281-288, 2005.

[72] C. S. Goldenstein, R. M. Spearrin, J. B. Jeffries *et al.*, "Infrared laser-absorption sensing for combustion gases," *Progress in Energy and Combustion Science,* vol. 60, pp. 132-176, 2017.
[73] A. Farooq, A. B. S. Alquaity, M. Raza *et al.*, "Laser sensors for energy systems and process industries: Perspectives and directions," *Progress in Energy and Combustion Science,* vol. 91, pp. 100997, 2022.
[74] W. Jing, Z. Cao, H. Zhang *et al.*, "A Reconfigurable Parallel Data Acquisition System for Tunable Diode Laser Absorption Spectroscopy Tomography," *IEEE Sensors Journal,* vol. 17, no. 24, pp. 8215-8223, 2017.
[75] F. Wang, Q. Wu, Q. Huang *et al.*, "Simultaneous measurement of 2-dimensional H2O concentration and temperature distribution in premixed methane/air flame using TDLAS-based tomography technology," *Optics Communications,* vol. 346, pp. 53-63, 2015.
[76] D. Wen, and Y. Wang, "Spatially and temporally resolved temperature measurements in counterflow flames using a single interband cascade laser," *Optics Express,* vol. 28, no. 25, pp. 37879-37902, 2020.
[77] Z. Wang, S. T. Sanders, J. A. Backhaus *et al.*, "H2O absorption tomography in a diesel aftertreatment system using a polymer film for optical access," *Applied Physics B,* vol. 123, no. 12, pp. 286, 2017.
[78] M. Raza, L. Ma, C. Yao *et al.*, "MHz-rate scanned-wavelength direct absorption spectroscopy using a distributed feedback diode laser at 2.3 μm," *Optics & Laser Technology,* vol. 130, pp. 106344, 2020.
[79] A. P. Nair, D. D. Lee, D. I. Pineda *et al.*, "MHz laser absorption spectroscopy via diplexed RF modulation for pressure, temperature, and species in rotating detonation rocket flows," *Applied Physics B,* vol. 126, no. 8, pp. 138, 2020.
[80] N. Q. Minesi, M. O. Richmond, C. C. Jelloian *et al.*, "Multi-line Boltzmann regression for near-electronvolt temperature and CO sensing via MHz-rate infrared laser absorption spectroscopy," *Applied Physics B,* vol. 128, no. 12, pp. 214, 2022.
[81] A. P. Nair, N. Minesi, C. Jelloian *et al.*, "Extended tuning of distributed-feedback lasers in a bias-tee circuit via waveform optimization for MHz-rate absorption spectroscopy," *Measurement Science and Technology,* vol. 33, no. 10, pp. 105104, 2022.
[82] A. P. Nair, N. Q. Minesi, C. Jelloian *et al.*, "RF-waveform optimization for MHz-rate DFB laser absorption spectroscopy in dynamic combustion environments," *AIAA SCITECH 2022 Forum*, AIAA SciTech Forum: American Institute of Aeronautics and Astronautics, 2021.
[83] Z. Wang, P. Fu, and X. Chao, "Laser Absorption Sensing Systems: Challenges, Modeling, and Design Optimization," *Applied Sciences,* vol. 9, no. 13, 2019.
[84] L. L. Röder, and H. Fischer, "Theoretical investigation of applicability and limitations of advanced noise reduction methods for wavelength modulation spectroscopy," *Applied Physics B,* vol. 128, no. 1, pp. 10, 2021.
[85] J. Li, B. Yu, W. Zhao *et al.*, "A Review of Signal Enhancement and Noise Reduction Techniques for Tunable Diode Laser Absorption Spectroscopy," *Applied Spectroscopy Reviews,* vol. 49, no. 8, pp. 666-691, 2014.
[86] G. Enemali, R. Zhang, H. McCann *et al.*, "Cost-Effective Quasi-Parallel Sensing Instrumentation for Industrial Chemical Species Tomography," *IEEE Transactions on Industrial Electronics,* vol. 69, no. 2, pp. 2107-2116, 2022.
[87] E. M. D. Fisher, S. Tsekenis, Y. Yang *et al.*, "A custom, high-channel count data acquisition system for chemical species tomography of aero-jet engine exhaust plumes," *IEEE Transactions on Instrumentation and Measurement,* vol. 69, no. 2, pp. 549 - 558, 2019.
[88] A. Huang, Z. Cao, W. Zhao *et al.*, "Frequency Division Multiplexing and Main Peak Scanning WMS Method for TDLAS Tomography in Flame Monitoring," *IEEE Transactions on Instrumentation and Measurement,* vol. 69, no. 11, pp. 9087-9096, 2020.
[89] L. Xu, R. Xue, Y. Li *et al.*, "FPGA-Based Real-Time Implementation of Temperature Measurement via Tunable Diode Laser Absorption Spectroscopy," *IEEE Sensors Journal,* vol. 18, no. 7, pp. 2751-2758, 2018.
[90] G. B. Rieker, J. B. Jeffries, and R. K. Hanson, "Calibration-free wavelength-modulation spectroscopy for measurements of gas temperature and concentration in harsh environments," *Appl. Opt.,* vol. 48, no. 29, pp. 5546-5560, 2009.

[91] A. Chighine, E. Fisher, D. Wilson *et al.*, "An FPGA-based lock-in detection system to enable Chemical Species Tomography using TDLAS," *2015 IEEE International Conference on Imaging Systems and Techniques (IST).* pp. 1-5, 2015.
[92] A. Huang, Z. Cao, C. Wang *et al.*, "An FPGA-based on-chip neural network for TDLAS tomography in dynamic flames," *IEEE Transactions on Instrumentation and Measurement,* vol. 70, no. 4506911, pp. 1-11, 2021.
[93] J. Xia, G. Enemali, R. Zhang *et al.*, "FPGA-Accelerated Distributed Sensing System for Real-Time Industrial Laser Absorption Spectroscopy Tomography at Kilo-Hertz," *Submitted to IEEE Transactions on Industrial Informatics*.
[94] G. Li, E. Dong, and W.-h. Ji, "A Near-Infrared Trace CO2 Detection System Based on an 1,580 nm Tunable Diode Laser Using a Cascaded Integrator Comb (CIC) Filter-Assisted Wavelength Modulation Technique and a Digital Lock-in Amplifier," *Frontiers in Physics,* vol. 7, pp. 199, 2019.
[95] W. Zhang, R. Zhang, Y. Fu *et al.*, "Machine Leaning Based Wavelength Modulation Spectroscopy for Rapid Gas Sensing," *2021 IEEE International Instrumentation and Measurement Technology Conference (I2MTC).* pp. 1-5, 2021.
[96] "Designing Distributed TSN Ethernet-Based Measurement Systems," https://www.ni.com/en-gb/innovations/white-papers/17/designing-distributed-tsn-ethernet-based-measurement-systems.html.
[97] N. Polydorides, A. Tsekenis, E. Fisher *et al.*, "Constrained models for optical absorption tomography," *Applied Optics,* vol. 57, no. 7, pp. B1-B9, 2018.
[98] S. J. Grauer, P. J. Hadwin, and K. J. Daun, "Improving chemical species tomography of turbulent flows using covariance estimation," *Applied Optics,* vol. 56, no. 13, pp. 3900-3912, 2017.
[99] S. J. Grauer, P. J. Hadwin, T. A. Sipkens *et al.*, "Measurement-based meshing, basis selection, and prior assignment in chemical species tomography," *Optics Express,* vol. 25, no. 21, pp. 25135-25148, 2017.
[100] C. Wei, K. K. Schwarm, D. I. Pineda *et al.*, "Physics-trained neural network for sparse-view volumetric laser absorption imaging of species and temperature in reacting flows," *Optics Express,* vol. 29, no. 14, pp. 22553-22566, 2021.
[101] J. Si, G. Fu, X. Liu *et al.*, "A Spatially Progressive Neural Network for Locally/Globally Prioritized TDLAS Tomography," *IEEE Transactions on Industrial Informatics*.
[102] M. Raissi, P. Perdikaris, and G. E. Karniadakis, "Physics-informed neural networks: A deep learning framework for solving forward and inverse problems involving nonlinear partial differential equations," *Journal of Computational Physics,* vol. 378, pp. 686-707, 2019.
[103] G. C. Mathews, and C. S. Goldenstein, "Wavelength-Modulation Spectroscopy for MHz Thermometry and H2O Sensing in Combustion Gases of Energetic Materials," *AIAA Scitech 2019 Forum*, AIAA SciTech Forum: American Institute of Aeronautics and Astronautics, 2019.
[104] R. S. M. Chrystie, E. F. Nasir, and A. Farooq, "Towards simultaneous calibration-free and ultra-fast sensing of temperature and species in the intrapulse mode," *Proceedings of the Combustion Institute,* vol. 35, no. 3, pp. 3757-3764, 2015.
[105] G. Duxbury, K. G. Hay, N. Langford *et al.*, "Real-time diagnostics of a jet engine exhaust using an intra-pulse quantum cascade laser spectrometer," *Molecular Physics,* vol. 109, no. 17-18, pp. 2131-2142, 2011.
[106] E. F. Nasir, and A. Farooq, "Time-resolved temperature measurements in a rapid compression machine using quantum cascade laser absorption in the intrapulse mode," *Proceedings of the Combustion Institute,* vol. 36, no. 3, pp. 4453-4460, 2017.
[107] E. F. Nasir, and A. Farooq, "Intra-pulse H2O absorption diagnostic for temperature sensing in a rapid compression machine," *Applied Physics B,* vol. 125, no. 11, pp. 210, 2019.
[108] R. K. Cole, A. S. Makowiecki, N. Hoghooghi *et al.*, "Baseline-free quantitative absorption spectroscopy based on cepstral analysis," *Optics Express,* vol. 27, no. 26, pp. 37920-37939, 2019.
[109] C. S. Goldenstein, G. C. Mathews, R. K. Cole *et al.*, "Cepstral analysis for baseline-insensitive absorption spectroscopy using light sources with pronounced intensity variations," *Applied Optics,* vol. 59, no. 26, pp. 7865-7875, 2020.

[110] J. Li, K. K. Schwarm, C. Wei *et al.*, "Robust cepstral analysis at variable wavelength scan depth for narrowband tunable laser absorption spectroscopy," *Measurement Science and Technology,* vol. 32, no. 4, pp. 045502, 2021.
[111] L. A. Kranendonk, X. An, A. W. Caswell *et al.*, "High speed engine gas thermometry by Fourier-domain mode-locked laser absorption spectroscopy," *Optics Express,* vol. 15, no. 23, pp. 15115-15128, 2007.
[112] L. Ma, and W. Cai, "Tomographic imaging of temperature and chemical species based on hyperspectral absorption spectroscopy," *Opt. Express,* vol. 17, no. 10, pp. 8602-8613, 2009.
[113] L. Ma, X. Li, S. T. Sanders *et al.*, "50-kHz-rate 2D imaging of temperature and H2O concentration at the exhaust plane of a J85 engine using hyperspectral tomography," *Opt. Express,* vol. 21, no. 1, pp. 1152-1162, 2013.
[114] W. Cai, and C. F. Kaminski, "A tomographic technique for the simultaneous imaging of temperature, chemical species, and pressure in reactive flows using absorption spectroscopy with frequency-agile lasers," *Applied Physics Letters,* vol. 104, no. 3, pp. 034101, 2014.
[115] T. Werblinski, P. Fendt, L. Zigan *et al.*, "High-speed combustion diagnostics in a rapid compression machine by broadband supercontinuum absorption spectroscopy," *Applied Optics,* vol. 56, no. 15, pp. 4443-4453, 2017.
[116] B. Niels Göran, E. Volker, D. Andreas *et al.*, "Broadband fitting approach for the application of supercontinuum broadband laser absorption spectroscopy to combustion environments," *Measurement Science and Technology,* vol. 27, no. 1, pp. 015501, 2016.
[117] T. Werblinski, S. Kleindienst, R. Engelbrecht *et al.*, "Supercontinuum based absorption spectrometer for cycle-resolved multiparameter measurements in a rapid compression machine," *Applied Optics,* vol. 55, no. 17, pp. 4564-4574, 2016.
[118] N. Göran Blume, and S. Wagner, "Broadband supercontinuum laser absorption spectrometer for multiparameter gas phase combustion diagnostics," *Optics Letters,* vol. 40, no. 13, pp. 3141-3144, 2015.
[119] S. J. Grauer, R. W. Tsang, and K. J. Daun, "Broadband chemical species tomography: Measurement theory and a proof-of-concept emission detection experiment," *Journal of Quantitative Spectroscopy and Radiative Transfer,* vol. 198, pp. 145-154, 2017.
[120] S. J. Grauer, J. Emmert, S. T. Sanders *et al.*, "Multiparameter gas sensing with linear hyperspectral absorption tomography," *Measurement Science and Technology,* vol. 30, no. 10, pp. 105401, 2019.
[121] L. Ma, and W. Cai, "Numerical investigation of hyperspectral tomography for simultaneous temperature and concentration imaging," *Appl. Opt.,* vol. 47, no. 21, pp. 3751--3759, 2008.
[122] W. Cai, and C. Kaminski, "A numerical investigation of high-resolution multispectral absorption tomography for flow thermometry," *Applied Physics B,* vol. 119, no. 1, pp. 29-35, 2015.